

# Geospatial Assessment of Flood Susceptibility in the Nong Peung Wetland, Central Laos

Vongphet Sihapanya<sup>1,2</sup>, Chittana Phompila<sup>1\*</sup>, Xinping Wen<sup>2</sup>, Kethsa Nongthavongduangsi<sup>1</sup>, Metmany Soukhavong<sup>1</sup>, Phomsanh Chantharangson<sup>1</sup>, Rajendra P. Shrestha<sup>3</sup>

<sup>1</sup>The Faculty of Forest Science, National University of Laos, Vientiane, Lao

<sup>2</sup>Faculty of Land Resource Engineering, Kunming University of Science and Technology, Kunming, China

<sup>3</sup>Natural Resources and Management, Department of Food, Agriculture, and Natural Resources, Asian Institute of Technology, Bangkok, Thailand

Email: \*c.phompila@nuol.edu.la

**How to cite this paper:** Sihapanya, V., Phompila, C., Wen, X.P., Nongthavongduangsi, K., Soukhavong, M., Chantharangson, P. and Shrestha, R.P. (2025) Geospatial Assessment of Flood Susceptibility in the Nong Peung Wetland, Central Laos. *Advances in Remote Sensing*, **14**, 221-240. <https://doi.org/10.4236/ars.2025.144014>

**Received:** October 16, 2025

**Accepted:** December 9, 2025

**Published:** December 12, 2025

Copyright © 2025 by author(s) and Scientific Research Publishing Inc. This work is licensed under the Creative Commons Attribution International License (CC BY 4.0).

<http://creativecommons.org/licenses/by/4.0/>



Open Access

## Abstract

Inundation events within the Nong Peung wetland of Pakxan district, Laos, represent a growing environmental and societal challenge, a threat compounded by the interplay of accelerated land use transformations, ongoing deforestation, and the broader impacts of climate change. This study presents the first systematic, geospatial assessment of flood susceptibility for this critical region, filling a significant void in local hazard analysis. We applied an integrated model utilizing a Geographic Information System (GIS) coupled with a Multi-Criteria Decision-Making (MCDM) approach, using the Analytical Hierarchy Process (AHP) for the systematic weighting of causative factors. The analysis incorporated nine determinative variables: elevation, slope, annual rainfall, proximity to river channels, drainage density, Topographic Wetness Index (TWI), land use/land cover, soil composition, and the Normalized Difference Vegetation Index (NDVI). The resultant susceptibility model stratifies the landscape into five classes, identifying 13.80% of the area as “very high risk” and 20.06% as “high risk.” Cumulatively, our model indicates that more than half (61.42%) of the wetland exhibits moderate to very high susceptibility to flooding. Areas of acute risk are concentrated in the northern and southern portions of the wetland, a spatial pattern directly attributable to a convergence of low elevation, gentle slopes, concentrated rainfall, high drainage density, and predominant agricultural land use. Validation against historical flood records confirms a strong predictive agreement, substantiating the reliability of the AHP-GIS framework for this application. The high-resolution susceptibility map produced by this research offers a foundational, evidence-based tool for enhancing disaster risk reduction strategies and guiding sustainable development in the Pakxan district.

---

## Keywords

Flood Susceptibility, Land Use Change, Hazard Assessment, Remote Sensing/GIS, Wetland Hydrology, Central Laos

---

## 1. Introduction

Natural hazards, particularly floods, represent one of the most serious global concerns confronting nations today [1]-[3]. Recognized worldwide as the most prevalent and destructive natural catastrophes [4] [5], floods are responsible for approximately 40% of all global socioeconomic losses [6]. Laos is exposed to a spectrum of natural hazards, including climatic, hydrological, and geological events that recurrently disrupt socio-economic stability. Among these, flooding, driven primarily by the Mekong River system and intensified by the annual southwest monsoon, constitutes the most pervasive and damaging natural hazard [6]-[9]. While seasonal inundation is a characteristic feature of the region, its frequency and severity are escalating due to climate change, leading to more frequent and intense typhoon events and alterations in rainfall patterns. These hydrologic events consistently threaten lives, damage critical infrastructure, and undermine essential services, with the central and southern provinces being particularly vulnerable. The human cost of these events is substantial; for instance, recent monsoon floods resulted in significant casualties and displaced over 150,000 people, with thousands of homes destroyed or damaged [7] [8].

This study focuses on the Nong Peung wetland within the Pakxan district of Bolikhamxay province, a region where a significant portion of the population is directly exposed to both floods and droughts. This wetland is socio-economically vital, encompassing 14 villages whose populations are heavily reliant on agriculture, particularly subsistence rice cultivation which dominates the local land use. These communities and associated residential settlements depend directly on the wetland's water resources, making their livelihoods acutely sensitive to hydrological disruptions. This deep socio-economic dependence on a flood-prone landscape reinforces the urgency of this assessment. Despite the documented susceptibility of the province, where flooding affects over 22% of the total area, a systematic, geospatial assessment of flood-prone areas has not been previously undertaken [6]-[9]. This research gap is critical, as the damages associated with flooding are projected to increase substantially due to ongoing socioeconomic development and climatic shifts. The Intergovernmental Panel on Climate Change (IPCC) has already projected an increased frequency of flood events in Southeast Asia, underscoring the urgency of proactive hazard assessment in developing nations like Laos [6] [8] [10].

Flood susceptibility mapping is a foundational component of effective disaster risk mitigation, providing decision-makers with the necessary tools to prioritize interventions and guide sustainable land-use planning [2] [4] [5] [11] [12]. In re-

cent years, the integration of Geographic Information Systems (GIS) with Multi-Criteria Decision Analysis (MCDA) has emerged as a robust methodology for spatial hazard assessment, particularly in data-limited environments [1] [2] [13]. Among MCDA techniques, the Analytic Hierarchy Process (AHP), developed by [14], is widely employed due to its systematic approach to weighting causative factors through pairwise comparisons. The synthesis of GIS and AHP provides a reliable and precise framework for delineating flood-prone zones by integrating diverse geospatial datasets [2] [4] [5] [11] [15].

Therefore, this research aims to develop the first comprehensive flood susceptibility map for the Nong Peung wetland, central Laos. By integrating multiple datasets—including elevation, slope, rainfall, distance to river, drainage density, Topographic Wetness Index (TWI), land use/land cover (LULC), soil type and vegetation cover—this study provides a vital tool for disaster management authorities. The specific objectives are:

- 1) To evaluate key climatic parameters and regional land use patterns using remote sensing data.
- 2) To delineate potential flood hazard zones by integrating a Multi-Criteria Decision-Making (MCDM) framework with the Analytical Hierarchy Process (AHP).
- 3) To validate the spatial flood susceptibility model against records of previous geo-hazard events.

## 2. Materials and Methods

### 2.1. Study Area

The study focuses on the Nong Peung wetland, located in the Pakxan district of Bolikhamxay province, central Laos (**Figure 1**). This area extends from 18°20'30.155"N to 18°25'21.162"N latitude and 103°38'9.033"E to 103°44'18.773"E longitude. The wetland covers approximately 63.85 Km<sup>2</sup>, at an elevation of 140 - 184 meters above sea level and encompasses 14 villages.

The region's hydro-climatology is dominated by a strong monsoon system that arrives in late July, leading to prolonged periods of intense rainfall. This precipitation frequently causes local rivers to exceed their bankfull capacity, resulting in widespread inundation of adjacent low-lying areas [7]. The specific topography of Pakxan town, combined with the hydrology of the Nong Peung wetland, makes the urban center particularly vulnerable to flooding.

The Nong Peung river system, which includes a network of lakes, ponds, canals, and marshes, supports a diverse ecosystem of aquatic and terrestrial species. It also serves as a critical water resource for surrounding communities, ultimately flowing into the Nam San and Mekong Rivers. Given the history of significant flood events in the area, a comprehensive flood risk assessment is essential for developing strategies to mitigate potential damage to local communities and infrastructure.

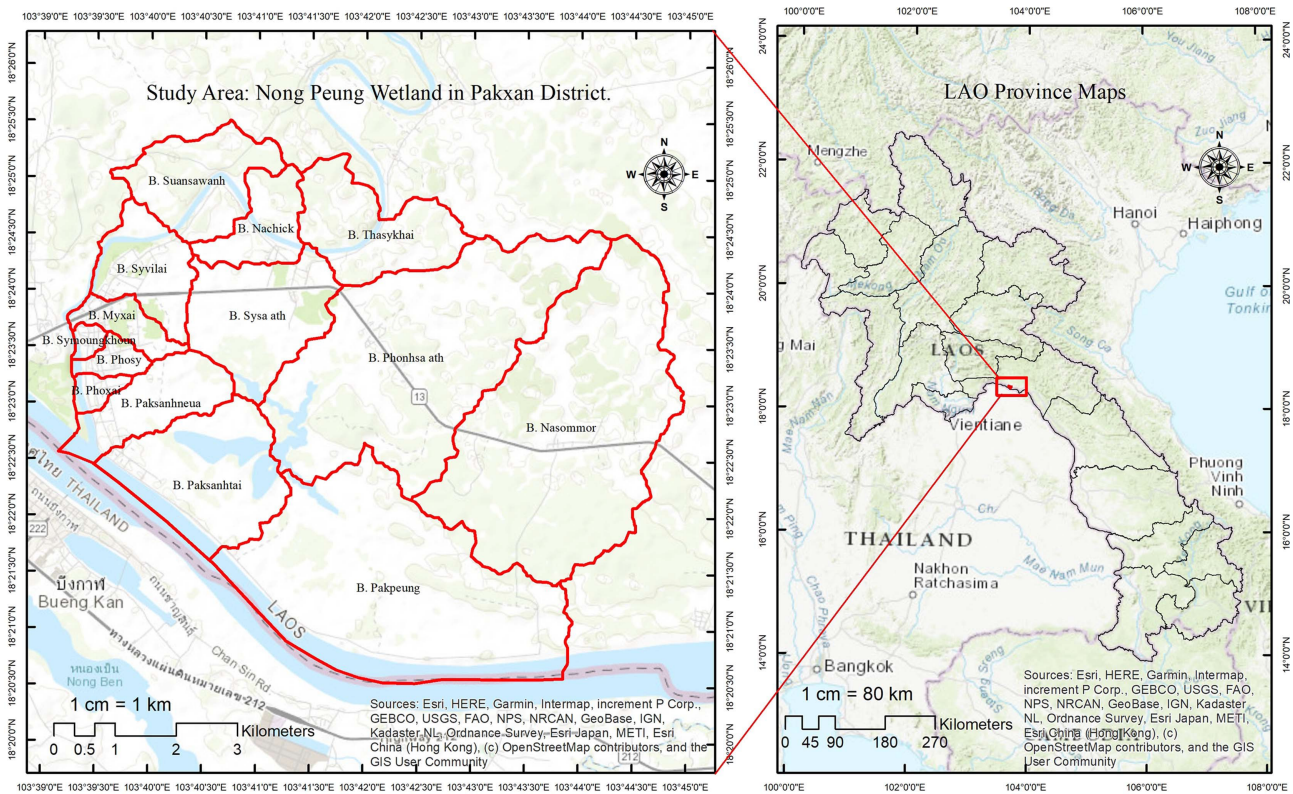


**Figure 1.** Study area Nong Peung Wetland in Pakxan District, Bolikhamxay Province, Laos.

## 2.2. Data Collection

The methodology for this study was contingent upon the acquisition and processing of multiple geospatial datasets to model urban flood risk. Nine parameters, identified as critical indicators of flood susceptibility through a comprehensive literature review, were derived from various sources (summarized in **Table 1**). The core datasets included:

**Topography:** A Digital Elevation Model (DEM) with a 30-meter spatial resolution was obtained from the USGS Earth Explorer. This was instrumental in generating essential topographic parameters, including elevation (EL), slope (SL), and the Topographic Wetness Index (TWI).

**Soil:** Soil type (ST) information was acquired from the Laos Digital Soil Map, a high-resolution (10 m) ESRI Shapefile provided by the Lao Knowledge for Development (<https://en.data.k4d.la>). Soil characteristics are a key determinant of surface runoff and infiltration rates.

**Land Use/Land Cover (LULC):** A high-resolution LULC map for 2023 was sourced from the Esri Land Cover collection within the ArcGIS Living Atlas. Derived from Sentinel-2A imagery, this dataset enabled the analysis of land use patterns, which significantly influence flood dynamics.

**Vegetation:** The Normalized Difference Vegetation Index (NDVI), a metric for vegetation health, was calculated from Sentinel-2A satellite imagery provided by the EU’s Copernicus program (<https://www.copernicus.eu/en>), acquired 24 April

2023.

**Hydrology:** Key hydrological factors, specifically distance to river (DR) and drainage density (DD), were derived from the DEM and existing hydrographic data.

**Precipitation:** Rainfall (Rf) data, a primary driver of flooding, was sourced from the high-resolution monthly and annual datasets provided by the Climate Research Unit, accessed via NASA POWER (<https://www.earthdata.nasa.gov>).

**Table 1.** Data types and brief description.

No	Data Types	Description	Data Sources
1	Digital Elevation Model (DEM)	Essential topographic information based on elevation and slope, 30 m of resolution	<a href="https://earthexplorer.usgs.gov/">https://earthexplorer.usgs.gov/</a> Digital Elevation-SRTM1 Arc-Second Global
2	Soil type	Information about Digital soil map of the district, scale of 1:250,000	<a href="https://www.k4d.la/">https://www.k4d.la/</a> Laos Knowledge for Development
3	Land use /Land cover (LULC) Map (2023)	Land use, along with patterns of land cover, is an important consideration. 10 m of resolution	Sentinel-2, accessed through Esri Land Cover-Arc GIS living Atlas <a href="https://livingatlas.arcgis.com/landcover/">https://livingatlas.arcgis.com/landcover/</a>
4	Vegetation Analysis (NDVI)	Insights into vegetation health analysis from the Sentinel-2A Satellite image, 10 m of resolution	<a href="https://browser.dataspace.copernicus.eu/">https://browser.dataspace.copernicus.eu/</a> the EU's Copernicus satellite Sentinel-2A (Acquired on 24 April 2023)
5	Precipitation Data	High-resolution precipitation (monthly and annually data from 2010-2022)	<a href="https://power.larc.nasa.gov/data-access-viewer/">https://power.larc.nasa.gov/data-access-viewer/</a>

The nine parameters selected for this study—encompassing critical geomorphological, hydrological, and land cover attributes—were chosen based on their established, direct influence on inundation dynamics. These factors (e.g., elevation, slope, rainfall, LULC) are widely validated in flood susceptibility literature as primary drivers of surface runoff and water accumulation, particularly within tropical, monsoon-driven wetland systems similar to the Nong Peung.

### 2.3. Data Analysis and Factor Map Preparation

All geospatial data were processed and analyzed using ArcGIS 10.8 to generate the nine thematic factor maps required for the Multi-Criteria Decision Analysis (MCDA). **Topographic and Hydrological Derivatives:** The DEM served as the primary source for several factors. It was first hydrologically corrected by filling sinks, from which flow direction and flow accumulation rasters were derived using the Hydrology toolset. The slope and curvature maps were calculated directly from the DEM. **Rainfall:** To create a continuous rainfall map, mean annual precipitation data from 14 local and regional meteorology stations (<https://www.earthdata.nasa.gov>) were interpolated using the Inverse Distance Weighted (IDW) method. The resulting raster was clipped to the study area boundary. **Drainage and Proximity:** The drainage network was delineated from

the flow accumulation raster, and this was used to compute the drainage density map via the Line Density tool. The distance to river map was generated by applying the Euclidean Distance tool to a river network layer sourced from the Lao Knowledge for Development (<https://en.data.k4d.la>). Topographic Wetness Index (TWI): The TWI map was generated using the Raster Calculator tool, applying the standard formula proposed by Moore *et al.* (1991) (Equation (1)).

$$W = Ln\left(\frac{A_s}{\tan B}\right) \quad (1)$$

where  $W$  represents the topographic wetness index,  $A_s$  represents the cumulative upslope area draining through a point (per unit contour length), and  $B$  represents the local slope angle in degrees.

To create the Land Use and Land Cover (LULC) factor map, we first extracted the LULC map of the district from the land use and land cover data available on the ESRI website. Next, we used ArcGIS software to assign appropriate names to each LULC class, as the downloaded map represents these classes by numbers.

To create the soil type factor map, we first identified the soil types of the watershed. This was done by extracting data using ArcGIS 10.8 software from the Digital Soil Map of Laos, which we obtained from the Lao Knowledge for Development. Once the soil types were extracted as a vector soil map, we converted it into raster format.

The NDVI map for the district was created using a Sentinel 2A satellite image, which was downloaded from the EU's Copernicus website. The map was generated by applying the equation provided below (Equation (2)) with ArcGIS 10.8 software.

$$NDVI = \frac{(NIR - RED)}{(NIR + RED)} = \frac{(Band\ 8 - Band\ 4)}{(Band\ 8 + Band\ 4)} \quad (2)$$

The NDVI, or Normalized Difference Vegetation Index, is calculated using surface spectral reflectance values. In this context, NIR refers to the reflectance in the near-infrared band, which corresponds to band 8 in the Sentinel 2A satellite imagery. RED refers to the reflectance in the red band, which is band 4 in the same satellite imagery.

After preparing all flood-controlling factors in raster format, we reclassified these factors into five common measurement scales ranging from 1 (very low susceptibility to flooding) to 5 (very high susceptibility to flooding). The data was rescaled to a consistent spatial resolution of 10 meters. A higher classification value (5) indicates areas that are more susceptible to flooding, while a lower value (1) corresponds to areas that are less susceptible. Since there is no standard reclassification scale for flood-controlling factors, the classification of all factors was determined based on previous studies and the local context of the study area.

Map Standardization and Flood Risk Modeling: Following their generation, all nine factor maps (El, Sl, Rf, DR, DD, TWI, LULC, ST, and NDVI) were standardized. Each map was reclassified into five flood susceptibility categories: Very Low

(1), Low (2), Moderate (3), High (4), and Very High (5). The area corresponding to each susceptibility level for every criterion is detailed in **Table 2**. All raster layers were subsequently resampled to a uniform spatial resolution of 10 meters. Finally, a weighted overlay analysis, integrating the factor weights derived from the Analytical Hierarchy Process (AHP), was performed to produce the final flood risk map for the Nong Peung wetland.

#### 2.4. Analysis Hierarchy Process (AHP)

The relative weights of the eleven factors influencing flood susceptibility in the Nong Peung wetland were derived using the Analytical Hierarchy Process (AHP). AHP is a multi-criterion decision-making (MCDM) method that systematically quantifies the relative importance of multiple criteria [1]-[4] [11] [12] [16]. The process involved three stages. First, a pairwise comparison matrix was constructed using Saaty's 1-to-9 scale to score the relative importance of one factor over another. Second, this matrix was normalized by dividing each element by its column total. Third, the final criteria weights were determined by calculating the row-wise average of the normalized matrix. To validate the judgments, the consistency of the matrix was evaluated. This required the calculation of the Consistency Index (CI) (Equation (3)) and the Consistency Ratio (CR) (Equation (4)).

$$CI = \frac{\lambda_{\max} - n}{n - 1} \quad (3)$$

$$CR = \frac{CI}{RI} \quad (4)$$

where  $n$  is the number of factors (11),  $\lambda_{\max}$  is the principal eigenvalue, and RI is the standard Random Index for  $n = 11$ . A CR value below the 0.10 threshold signifies that the matrix judgments are consistent and acceptable (Saaty 1987).

To ensure a transparent weighting process, the pairwise comparison judgments were derived from a hybrid approach. This involved: 1) a comprehensive review of established flood susceptibility literature to determine the general importance of factors, and 2) a consensus of the authors' expert judgment to adapt these principles to the specific hydrological context of the Nong Peung wetland.

#### 2.5. Flood Susceptibility Mapping

After preparing and reclassifying each flood-controlling factor to a common measurement scale ranging from 1 (very low) to 5 (very high) using ArcGIS software, we then applied the Analytic Hierarchy Process (AHP) to weight these factors. Subsequently, the spatial layers were integrated and overlaid together in the Spatial Analyst Extension of the ArcGIS environment using the weighted overlay technique. We employed the equation (Equation (5)) presented below to derive the flood susceptibility map of the study area. Several previous studies [1]-[5] [11] [12] [15]-[17] have utilized this equation (Equation (5)) to generate flood susceptibility maps.

$$FS = \sum_{i=0}^n x_i * w_i \quad (5)$$

In this context, (FS) represents flood susceptibility, ( $n$ ) denotes the number of decision criteria, ( $x_i$ ) refers to a specific normalized criterion, and ( $w_i$ ) indicates the corresponding weight assigned to that criterion. The values of each cell or pixel in the raster layers are multiplied by their respective weights, which are derived from AHP (Analytic Hierarchy Process) analysis. These weighted values are then summed together to produce the flood susceptibility output raster map.

## 2.6. Model Validation

To assess the predictive accuracy of the generated Flood Susceptibility Map (FSM), a validation process was conducted using an independent dataset of known flood locations. A flood inventory map was prepared comprising 45 “Flood plain samples”. These locations were identified based on historical inundation records obtained from the Pakxan District Agricultural and Forestry Office (DAFO) and supplemented by field-based GPS surveys conducted in 2023.

The validation was performed by spatially correlating this inventory of known flood points with the five susceptibility classes (Very Low to Very High) of the final FSM. The model’s reliability is confirmed by the high concentration of these validation points falling within the areas classified as ‘High’ and ‘Very High’ susceptibility. Furthermore, to quantitatively measure the model’s performance, the Receiver Operating Characteristic (ROC) curve was employed [18]. The Area Under the Curve (AUC) was calculated, which provides a robust measure of the model’s ability to correctly distinguish between flood-prone and non-flood-prone areas.

## 3. Results

### 3.1. Spatial Distribution of Flood Conditioning Factors

The spatial analysis identified the distribution and characteristics of the nine factors conditioning flood susceptibility across the Nong Pueng wetland. The reclassified thematic maps revealed significant spatial heterogeneity, with each factor contributing differently to the overall flood risk. A detailed breakdown of each factor’s contribution is provided below, with quantitative data on area and percentage coverage presented in **Table 2**.

**Elevation:** The topography of the study area ranges from 140 m to 184 m. The reclassified Digital Elevation Model (DEM) shows a clear distinction between higher-elevation upstream areas and low-lying downstream plains (**Figure 2(a)**). Areas classified with ‘Very High’ susceptibility (140 - 151 m) are concentrated in these downstream regions, which are prone to water accumulation. Conversely, the ‘Very Low’ susceptibility class (169 - 184 m) corresponds to the highest ground, primarily in the upper catchment.

**Slope:** The slope analysis indicates that a substantial portion of the watershed is characterized by gentle terrain, which facilitates water stagnation. A total of

30.56% of the area (19.22 ha) has a slope of  $0^\circ - 2.5^\circ$ , falling into the ‘Very High’ susceptibility class (**Figure 2(b)**). These flat areas are predominantly located in the northeastern, central, and southwestern parts of the study area. In contrast, areas with low to very low susceptibility (slope  $> 8.7^\circ$ ) constitute only a small fraction of the landscape (8.54%).

**Rainfall:** Mean annual rainfall varies considerably, from 955 mm to 2380 mm. The ‘High’ (1830 - 2060 mm) and ‘Very High’ (2070 - 2380 mm) susceptibility classes collectively cover nearly half of the study area (47.33%). Spatially, the western parts of the region receive the highest precipitation volumes, rendering them more vulnerable to rainfall-induced flooding compared to the eastern parts (**Figure 2(c)**).

**Distance from river:** Proximity to the river network is a critical determinant of flood risk. The analysis shows that areas within 130 m of a river channel are classified as ‘Very Highly’ susceptible to inundation. These high-risk zones are concentrated along the primary river corridors and their immediate floodplains (**Figure 2(d)**). As distance from the river increases, the susceptibility level decreases, with areas over 620 m away classified as having ‘Very Low’ susceptibility.

**Table 2.** Flood conditioning factors, their classification, rating values, area coverage, and percentage.

Factor	Classes	Food Susceptibility	Rating	Area	
				Km <sup>2</sup>	Percent (%)
Elevation (El) (m)	140 - 151	Very High	5	4.96	7.77
	152 - 156	High	4	14.85	23.25
	157 - 161	Moderate	3	18.43	28.87
	162 - 168	Low	2	20.40	31.94
	169 - 184	Very Low	1	5.22	8.17
Slope (degree)	0 - 2.5	Very High	5	0.82	1.31
	2.6 - 5.2	High	4	4.70	7.48
	5.3 - 8.6	Moderate	3	14.08	22.39
	8.7 - 14	Low	2	24.05	38.26
	15 - 38	Very Low	1	19.21	30.56
Rainfall (mm/year)	955 - 1.300	Very low	1	7.95	12.45
	1.340 - 1.570	Low	2	11.28	17.67
	1.580 - 1.820	Moderate	3	14.40	22.55
	1.830 - 2.060	High	4	25.27	39.58
	2.070 - 2.382	Very High	5	4.95	7.75
Distance from river (m)	0 - 132	Very High	5	3.68	5.77
	133 - 280	High	4	9.20	14.4
	281 - 432	Moderate	3	13.25	20.75

## Continued

	433 - 605	Low	2	17.35	27.17
	606 - 1.050	Very Low	1	20.38	31.91
Drainage Density (km/km <sup>2</sup> )	0 - 2.24	Very Low	1	38.10	59.74
	2.25 - 6.47	Low	2	14.91	23.39
	6.48 - 11.5	Moderate	3	4.51	7.08
	11.6 - 17.9	High	4	4.60	7.22
	18 - 30	Very High	5	1.64	2.58
Topographic Wetness Index (TWI)	-7.07 - -4.06	Very Low	1	26.98	42.26
	-4.05 - -1.95	Low	2	14.46	22.65
	-1.94 - 0.283	Moderate	3	10.37	16.25
	0.284 - 3.10	High	4	9.96	15.60
	3.11 - 9.23	Very High	5	2.07	3.25
Land use and land cover (LULC)	Waterbody	Very High	5	0.004	0.01
	Trees/Corps	High	4	2.48	3.9
	Built area/Rang Land	Moderate	3	12.22	19.14
	Flood Vegetation	Low	2	43.29	67.8
	Bare ground	Very Low	1	5.84	9.16
Soil Type	(ACf)/(LVg)	Very Low	1	0.74	1.15
	(CMd)/(ALg)	Low	2	10.53	16.52
	(ALf)/(LVf)	Moderate	3	13.84	21.73
	(ACg)	High	4	15.78	24.78
	(CMe)/(CMg)	Very High	5	22.81	35.81
Normalize Difference vegetation index NDVI	-0.6 - 0.068	Very High	5	12.47	19.53
	0.069 - 0.2	High	4	13.47	21.1
	0.21 - 0.3	Moderate	3	17.16	26.88
	0.31 - 0.4	Low	2	16.52	25.88
	0.41 - 0.58	Very Low	1	4.21	6.6

Drainage Density: The highest drainage densities (18 - 30 km/km<sup>2</sup>) correlated with 'Very High' susceptibility, impacting 2.58% of the area (**Figure 3(a)**). The lowest densities (0 - 2.24 km/km<sup>2</sup>) had 'Very Low' susceptibility and covered the majority of the study area (59.74%).

Topographic Wetness Index (TWI): Areas with the highest TWI values (3.11 - 9.23), indicating a high potential to accumulate water, corresponded to 'Very High' susceptibility (3.25% of area). The lowest TWI values (-7.07 - -4.06) were rated 'Very Low' (42.26%) (**Figure 3(b)**).

Land Use and Land Cover (LULC): 'Waterbody' was identified as the 'Very

High' susceptibility class, though it comprised only 0.01% of the area. 'Bare ground' was classified as 'Very Low' susceptibility (9.16%) (Figure 3(c)).

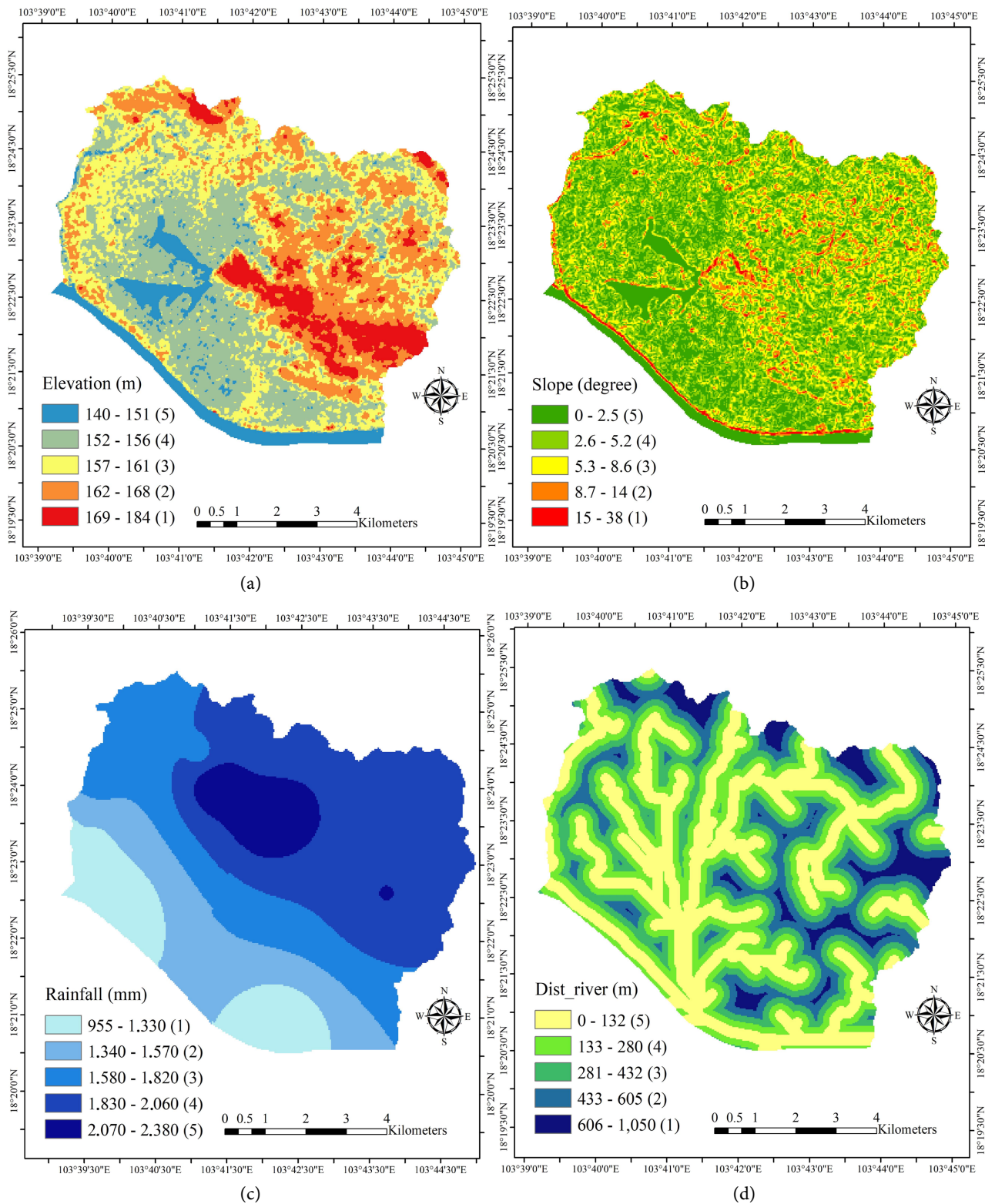


Figure 2. (a) Elevation; (b) Slope; (c) Rainfall; (d) Distance from river maps.

NDVI: The Normalized Difference Vegetation Index (NDVI) results showed that the lowest values ( $-0.6 - 0.068$ ), indicative of sparse vegetation or water, had ‘Very High’ susceptibility (19.53% of area) (Figure 4(a)). Conversely, the highest NDVI values ( $0.41 - 0.58$ ), representing dense vegetation, had ‘Very Low’ susceptibility (6.6%).

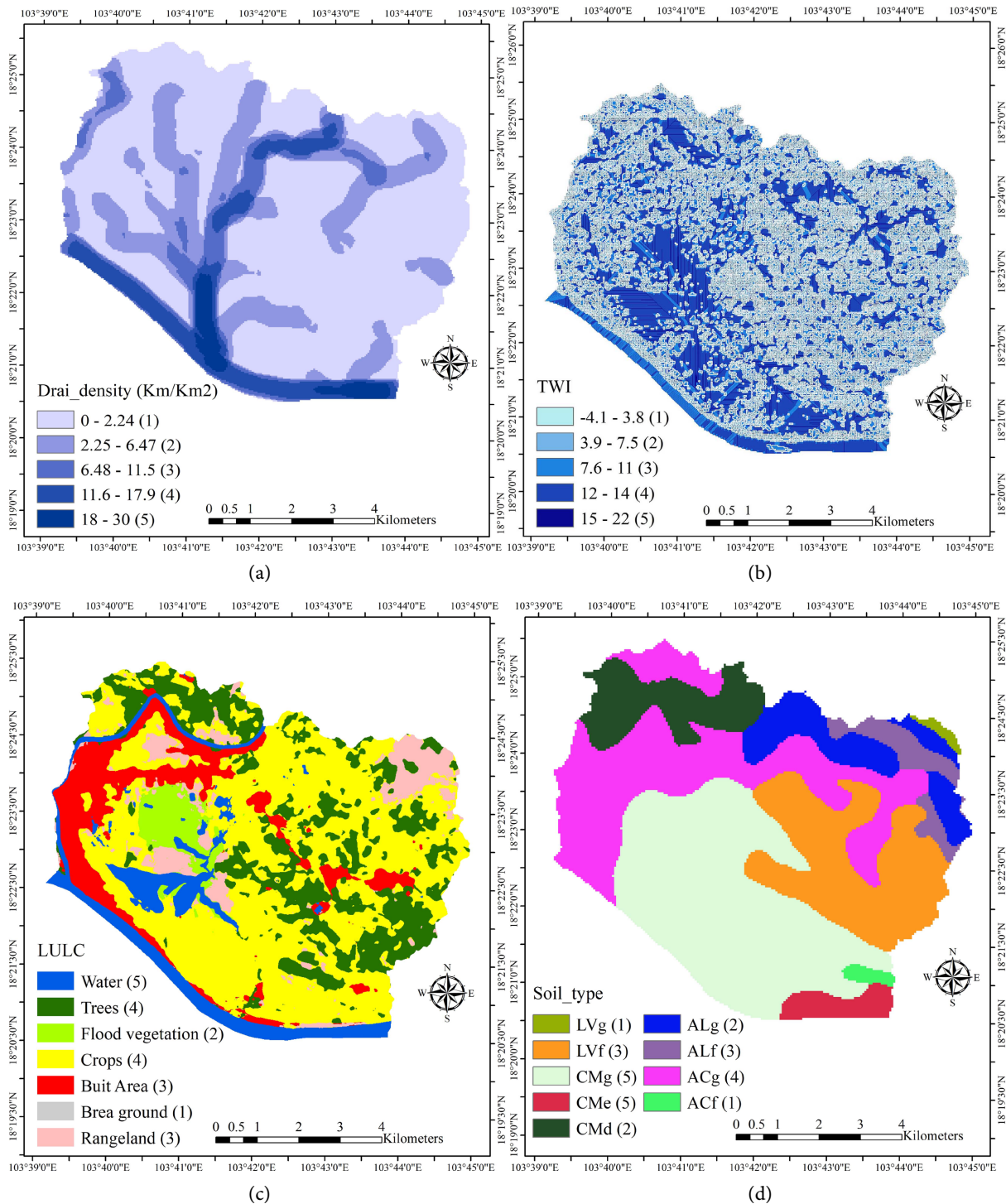


Figure 3. (a) Drainage density; (b) Topography witness index; (c) Land use land cover; (d) Soil type.

Soil Type: The (CMe)/(CMg) soil class showed ‘Very High’ susceptibility and was the most dominant high-susceptibility class, covering 35.81% of the study area. The (ACf)/(LVg) soil type was rated ‘Very Low’ (1.15%) (Figure 3(d)). It seems the highest flood susceptibility was consistently associated with low elevations, flat slopes, proximity to rivers, high rainfall, high drainage density, high TWI values, water bodies, (CMe)/(CMg) soil types, and low NDVI values.

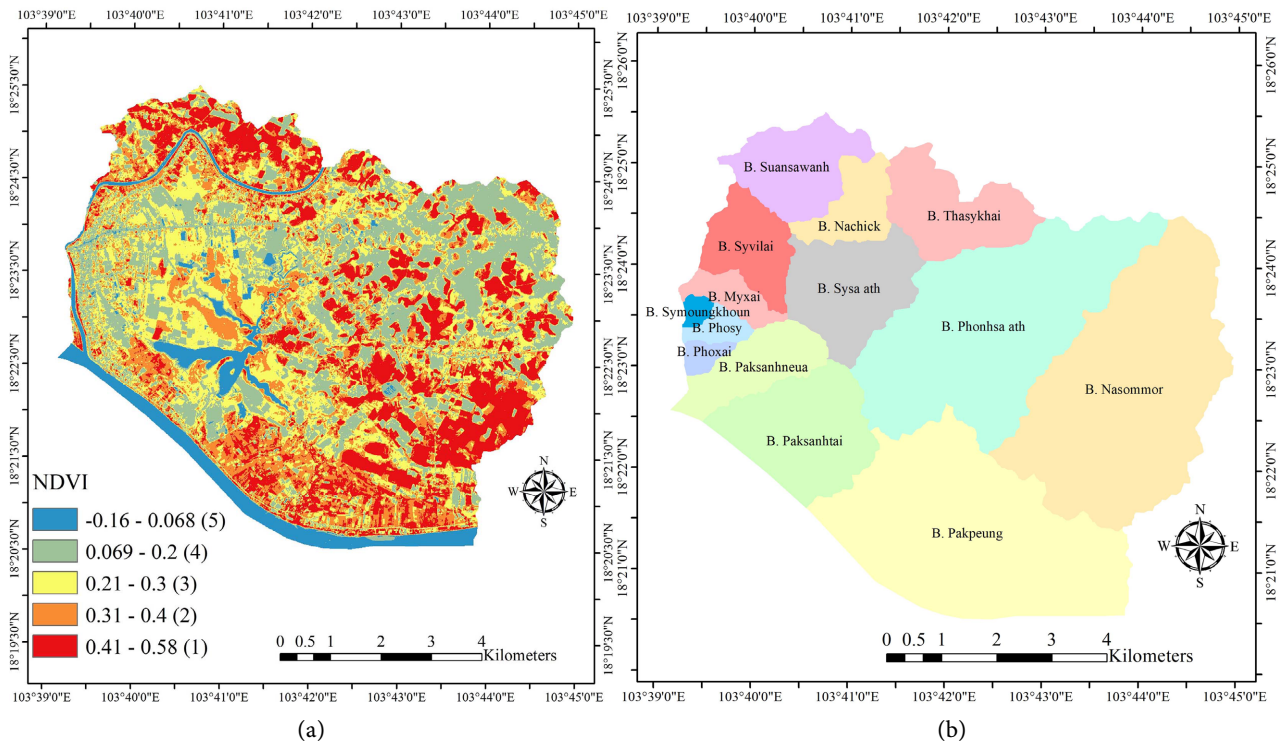


Figure 4. (a) Normalized different vegetation index (NDVI), (b) Villages around Nong-Peung wetland.

### 3.2. Factor Weighting and Model Consistency

The final weights for the nine flood-controlling factors, derived from the AHP pairwise comparison (Tables 3-5), quantify their relative influence on flood susceptibility. The results indicate that geomorphological characteristics are the primary drivers of flooding in the study area. Slope (24.35%) and elevation (21.92%) received the highest weights, collectively accounting for over 46% of the model's influence. This suggests that low-lying, flat terrain is the most critical condition for inundation. Hydrological factors, including annual rainfall (15.56%) and distance from rivers (13.83%), also showed significant influence. In contrast, surface and soil characteristics such as LULC (4.36%), soil type (2.67%), and NDVI (2.49%) had the lowest relative importance. A consistency check (Table 5) was performed to validate the AHP matrix. The resulting Consistency Ratio (CR) was 0.074 (7.4%), derived from a Consistency Index (CI) of 0.11 and a Random Index (RI) of 1.46 for  $n = 9$ . As this CR value is well below the 0.10 threshold stipulated by Saaty (1987), the pairwise judgments were deemed consistent and reliable for

use in the weighted overlay.4.2. Flood Susceptibility Map (FSM) Analysis. The final Flood Susceptibility Map (FSM) was generated by integrating the nine thematic factor maps using the AHP-derived weights. The FSM categorizes the Nong Peung wetland into five susceptibility classes, with their areal distribution detailed in **Table 5**. A key finding is that a majority of the study area, 61.4% (totaling 39.22 Km<sup>2</sup>), is classified as having ‘Moderate’ (27.56%), ‘High’ (20.06%), or ‘Very High’ (13.80%) susceptibility to flooding. The remaining 38.58% of the area exhibits ‘Low’ (24.84%) or ‘Very Low’ (13.74%) susceptibility. Spatially, the FSM (**Figure 5**) reveals that the most vulnerable areas are concentrated in the northern, western, central, and southern regions of the district. This spatial pattern is logical, as these areas correspond to the low-lying (low elevation) and flat (low slope) regions, which were the two most heavily weighted factors in the model. This confluence of high-risk geomorphology and proximity to drainage networks creates significant susceptibility to inundation.

**Table 3.** Estimated areas of flood susceptibility within the study area.

Flood Susceptibility	Rating	Area	
		Km <sup>2</sup>	Percent (%)
Very Low	1	8.77	13.74
Low	2	15.86	24.84
Moderate	3	17.60	27.56
High	2	12.81	20.06
Very High	1	8.81	13.80
<b>Total</b>		<b>63.85</b>	<b>100</b>

The results indicate that several areas are particularly vulnerable to flooding (**Table 3**). These include: B. Thasykhai, B. Nachick, B. Sysa ath, and B. Phonehsa ath in the northern part; B. Syvilai, B. Myxai, B. Symoungkhoun, B. Phosy, B. Phoxai, B. Pakxanhneua, and B. Pakxantai in the western part; B. Phonhsa ath also in the central part; B. Nasommor in the eastern part and B. Pakpeung in the southern part. These areas were identified as the most vulnerable to flooding within the study area. The analysis of flood susceptibility, as shown in (**Figure 5**), reveals that the areas of B. Sysaath, B. Phonhsath, B. Pakxanhneua, B. Pakxantai, and B. Pakpeung, located in the western, central, and southern parts of the district, are the most vulnerable to flooding.

#### 4. Discussions

This study was initiated to address a critical gap in the scientific literature and regional hazard management: the absence of a systematic, geospatial flood susceptibility assessment for the Nong Peung wetland in central Laos. Despite being a region recurrently affected by severe flooding, as documented by national and

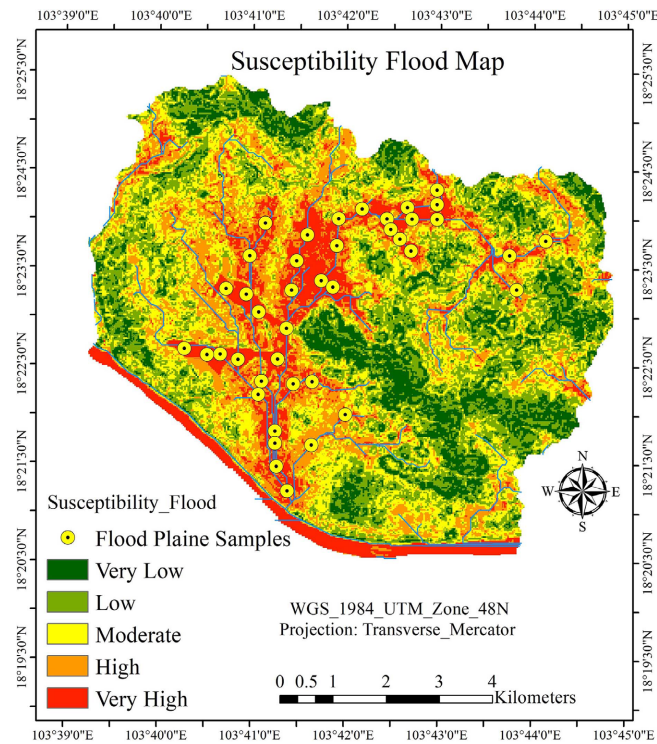


Figure 5. Susceptibility flood map of the study area.

Table 4. Normalized pairwise comparison matrix and calculated criteria weight for each factor.

Factors	Elevation	Slope	Rainfall	Distance to rivers	Drainage density	TWI	LULC	Soil type	NDVI	sum	Criteria Weight	Criteria weight %
Elevation	0.25	0.27	0.35	0.32	0.16	0.13	0.20	0.19	0.11	1.97	0.22	21.92
Slope	0.25	0.27	0.35	0.22	0.24	0.26	0.24	0.19	0.19	2.19	0.24	24.35
Rainfall	0.08	0.09	0.12	0.22	0.24	0.22	0.17	0.11	0.16	1.40	0.16	15.56
Distance to rivers	0.08	0.13	0.06	0.11	0.16	0.22	0.14	0.16	0.19	1.24	0.14	13.83
Drainage density	0.12	0.09	0.04	0.05	0.08	0.09	0.14	0.11	0.08	0.80	0.09	8.84
TWI	0.08	0.04	0.02	0.02	0.04	0.04	0.07	0.11	0.11	0.54	0.06	5.97
LULC	0.04	0.04	0.02	0.03	0.02	0.02	0.03	0.11	0.08	0.39	0.04	4.36
Soil type	0.04	0.04	0.03	0.02	0.02	0.01	0.01	0.03	0.05	0.24	0.03	2.67
NDVI	0.06	0.04	0.02	0.02	0.03	0.01	0.01	0.01	0.03	0.22	0.02	2.49

Table 5. Calculating the consistency of pairwise comparison (CR = 0.07).

Factors	Elevation	Slope	Rainfall	Distance to rivers	Drainage density	TWI	LULC	Soil type	NDVI	Weight sum value	criteria weight	WSV/CW
Elevation	0.22	0.24	0.47	0.41	0.18	0.18	0.26	0.19	0.10	2.25	0.22	10.26
Slope	0.22	0.24	0.47	0.28	0.27	0.36	0.31	0.19	0.17	2.50	0.24	10.25
Rainfall	0.07	0.08	0.16	0.28	0.27	0.30	0.22	0.11	0.15	1.62	0.16	10.44

**Continued**

Distance to rivers	0.07	0.12	0.08	0.14	0.18	0.30	0.17	0.16	0.17	1.40	0.14	10.09
Drainage density	0.11	0.08	0.05	0.07	0.09	0.12	0.17	0.11	0.07	0.88	0.09	9.91
TWI	0.07	0.04	0.03	0.03	0.04	0.06	0.09	0.11	0.10	0.57	0.06	9.54
LULC	0.04	0.03	0.03	0.03	0.02	0.03	0.04	0.11	0.07	0.41	0.04	9.49
Soil type	0.03	0.03	0.04	0.02	0.02	0.01	0.01	0.03	0.05	0.25	0.03	9.45
NDVI	0.05	0.03	0.03	0.02	0.03	0.01	0.01	0.01	0.02	0.23	0.02	9.35

international agencies [6]-[9], planning and mitigation efforts have been hampered by a lack of granular, evidence-based data. Our research provides the first comprehensive flood susceptibility map for this vital area, transitioning from broad-scale national reports to a localized, actionable tool for policymakers. By employing an integrated GIS and AHP-based MCDM framework, we have systematically quantified and mapped the spatial dimensions of flood risk, a methodology proven effective in similar data-scarce environments [10] [13] [15] [19]-[21]. Our analysis reveals that the Nong Peung wetland is inherently susceptible to flooding, with over 61% of its area classified as having moderate to very high susceptibility. The key finding of this study is the overwhelming influence of geomorphological factors on flood susceptibility. The AHP model assigned the highest weights to slope (24.35%) and elevation (21.92%), which collectively account for nearly half of the model's predictive power. This quantitatively confirms that the low-lying, gentle terrain of the wetland is the principal condition predisposing it to inundation. This is spatially manifested in the final susceptibility map, where high and very high-risk zones are concentrated in the northern, western, and southern regions, corresponding directly to areas with the lowest elevation and flattest slopes. Hydrological factors, particularly annual rainfall (15.56%) and proximity to river channels (13.83%), were identified as the next most significant drivers. This is consistent with the hydro-climatological context of the region, which is dominated by the southwest monsoon and the hydrology of the Mekong River system. In contrast, factors such as LULC (4.36%) and soil type (2.67%) received lower weights. While important, their influence appears secondary to the fundamental topographic and hydrological controls in this specific landscape. The results of this study are in strong agreement with the broader body of research on flood hazard mapping. The dominance of topography and hydrology as primary drivers of flood events is a well-established principle [22]. For example, studies conducted in other monsoon-driven river basins across Southeast Asia have similarly identified elevation, slope, and proximity to drainage networks as the most critical determinants of flood risk. Furthermore, our successful application of the AHP-GIS integrated approach corroborates its utility as a robust and cost-effective methodology for hazard assessment, as demonstrated by numerous international studies [2] [4] [5] [10] [12]-[14] [16] [17] [23]. The consistency of our find-

ings with established literature lends high confidence to the validity of the generated susceptibility map. While this study provides a robust foundational assessment, several limitations should be acknowledged. Firstly, the analysis relied on a DEM with a 30-meter spatial resolution. While sufficient for a regional overview, higher-resolution data (e.g., from LiDAR or drone-based surveys) could reveal more localized topographic features that influence water flow and accumulation, thereby refining the delineation of risk zones. Secondly, the rainfall data was interpolated from regional stations; this approach may not fully capture microclimatic variations within the wetland that could affect flood intensity. Thirdly, the AHP methodology, while systematic, incorporates a degree of subjectivity in the pairwise comparison process. Although our Consistency Ratio (CR = 0.074) was well within the acceptable threshold, the weighting is based on expert judgment and a review of existing literature rather than direct physical modeling. Finally, this assessment provides a static snapshot of susceptibility. It does not dynamically model the hydraulic and hydrological processes of a specific flood event, nor does it incorporate socio-economic factors that are critical for a comprehensive susceptibility assessment. This research lays the groundwork for several future research avenues and has direct implications for disaster risk management in the Pakxan district. We recommend future studies focus on integrating dynamic hydrological models (e.g., HEC-RAS) to simulate flood inundation depth and velocity for specific rainfall scenarios, which would complement the static susceptibility map produced here. Further research should also aim to incorporate socio-economic vulnerability by integrating data on population density, infrastructure, and livelihood strategies to transition from a hazard susceptibility map to a holistic flood risk map. For policymakers and planners, the high-resolution map presented in this study is an immediately applicable tool. It can guide the development of land-use zoning regulations to restrict critical infrastructure development in high-risk areas. Furthermore, it allows for the strategic prioritization of mitigation measures, such as the construction of levees or the enhancement of early warning systems, in the most vulnerable communities, particularly in B. Sysaath, B. Phonhsath, and the Pakxan urban area.

## 5. Conclusion

This study addressed the significant flood hazard in the NongPueng wetland, located in the Pakxan district of central Laos, by developing a comprehensive flood susceptibility map. The methodology integrated a GIS-based Multi-Criteria Decision-Making (MCDM) framework with the Analytical Hierarchy Process (AHP) to systematically evaluate nine key flood-conditioning factors, including elevation, slope, rainfall, drainage density, and land use/land cover (LULC). The analysis revealed that a substantial portion of the study area is highly vulnerable to flooding. A combined 33.85% of the region was classified as having 'High' (20.06%) or 'Very High' (13.80%) susceptibility, with an additional 27.56% falling into the 'Moderate' category. These high-risk zones were predominantly charac-

terized by a combination of low elevations, gentle slopes, high rainfall, high drainage density, specific agricultural land uses (cropland), and close proximity to river networks. Spatially, these vulnerable areas are concentrated in the northern, western, central, and southern parts of the study region, directly impacting numerous communities surrounding the wetland. The model's validity was confirmed through a strong correlation between the generated susceptibility map and the spatial distribution of historical flood events. This study confirms that the integrated AHP-GIS approach is a robust, cost-effective, and efficient tool for flood hazard assessment, particularly in regions where detailed hydrological data may be limited. The resulting map serves as a critical resource for policymakers and urban planners, providing an essential scientific basis for targeted flood risk management, improved land-use planning, and the prioritized implementation of mitigation strategies in the Pakxan district, central Laos.

### Acknowledgements

The authors gratefully acknowledge the U.S. Geological Survey (USGS) for providing open access to the Digital Elevation Model (DEM) and the Environmental Systems Research Institute (Esri) for the land use/land cover (LULC) map and Sentinel 2A satellite imagery. We also thank NASA's Prediction for Worldwide Energy Resources (<https://www.earthdata.nasa.gov>) for rainfall data and the Lao Knowledge for Development for soil type data (<https://en.data.k4d.la>). We extend our sincere appreciation to the Pakxan District Agricultural and Forestry Office (DAFO) and the Department of Natural Resources and Environment (DNRE) for their cooperation and for providing essential local information.

### Funding

This research was funded by the Urban EbS Knowledge-Hub at the Faculty of Forest Sciences (FFS), National University of Laos (NUoL).

### Conflicts of Interest

The authors declare no conflicts of interest regarding the publication of this paper.

### References

- [1] Ajjur, S.B. and Mogheir, Y.K. (2020) Flood Hazard Mapping Using a Multi-Criteria Decision Analysis and GIS (Case Study Gaza Governorate, Palestine). *Arabian Journal of Geosciences*, **13**, Article No. 44. <https://doi.org/10.1007/s12517-019-5024-6>
- [2] Allafta, H. and Opp, C. (2021) GIS-Based Multi-Criteria Analysis for Flood Prone Areas Mapping in the Trans-Boundary Shatt Al-Arab Basin, Iraq-Iran. *Geomatics, Natural Hazards and Risk*, **12**, 2087-2116. <https://doi.org/10.1080/19475705.2021.1955755>
- [3] Arseni, M., Rosu, A., Calmuc, M., Calmuc, V.A., Iticescu, C. and Georgescu, L.P. (2020) Development of Flood Risk and Hazard Maps for the Lower Course of the Siret River, Romania. *Sustainability*, **12**, Article No. 6588. <https://doi.org/10.3390/su12166588>

- [4] Aydin, M.C. and Sevgi Birincioglu, E. (2022) Flood Risk Analysis Using Gis-Based Analytical Hierarchy Process: A Case Study of Bitlis Province. *Applied Water Science*, **12**, Article No. 122. <https://doi.org/10.1007/s13201-022-01655-x>
- [5] Chakraborty, S. and Mukhopadhyay, S. (2019) Assessing Flood Risk Using Analytical Hierarchy Process (AHP) and Geographical Information System (GIS): Application in Coochbehar District of West Bengal, India. *Natural Hazards*, **99**, 247-274. <https://doi.org/10.1007/s11069-019-03737-7>
- [6] WBG-ADB (2021) Climate Risk Country Profile: Lao PDR.
- [7] IACP (2023) Inter-Agency Contingency Plan: Lao PDR.
- [8] UN-HABITAT (2023) Lao PDR Country Report 2023.
- [9] GoL (2018) The Post-Disaster Needs Assessment (PDNA).
- [10] Roberts, T., Parker, D.M., Bulterys, P.L., Rattanavong, S., Elliott, I., Phommasone, K., et al. (2021) A Spatio-Temporal Analysis of Scrub Typhus and Murine Typhus in Laos; Implications from Changing Landscapes and Climate. *PLOS Neglected Tropical Diseases*, **15**, e0009685. <https://doi.org/10.1371/journal.pntd.0009685>
- [11] Abdelkarim, A., Al-Alola, S.S., Alogayell, H.M., Mohamed, S.A., Alkadi, I.I. and Ismail, I.Y. (2020) Integration of GIS-Based Multicriteria Decision Analysis and Analytical Hierarchy Process to Assess Flood Hazard on the Al-Shamal Train Pathway in Al-Qurayyat Region, Kingdom of Saudi Arabia. *Water*, **12**, Article No. 1702. <https://doi.org/10.3390/w12061702>
- [12] Mukherjee, R. and Deb, P. (2023) Application of GIS-Based Analytical Hierarchy Process for Assessment and Mapping of Flood Risk Zone in the Lower Ramganga River Basin, Western Gangetic Plain, India. *Environment, Development and Sustainability*, **26**, 6163-6193. <https://doi.org/10.1007/s10668-023-02957-z>
- [13] Osman, S.A. and Das, J. (2023) Gis-based Flood Risk Assessment Using Multi-Criteria Decision Analysis of Shebelle River Basin in Southern Somalia. *SN Applied Sciences*, **5**, Article No. 134. <https://doi.org/10.1007/s42452-023-05360-5>
- [14] Saaty, T.L. (1990) How to Make a Decision: The Analytic Hierarchy Process. *European Journal of Operational Research*, **48**, 9-26. [https://doi.org/10.1016/0377-2217\(90\)90057-i](https://doi.org/10.1016/0377-2217(90)90057-i)
- [15] Das, S. and Pardeshi, S.D. (2017) Comparative Analysis of Lineaments Extracted from Cartosat, SRTM and ASTER DEM: A Study Based on Four Watersheds in Konkan Region, India. *Spatial Information Research*, **26**, 47-57. <https://doi.org/10.1007/s41324-017-0155-x>
- [16] Pimenta, L., Duarte, L., Teodoro, A.C., Beltrão, N., Gomes, D. and Oliveira, R. (2025) Gis-based Flood Susceptibility Mapping Using AHP in the Urban Amazon: A Case Study of Ananindeua, Brazil. *Land*, **14**, Article No. 1543. <https://doi.org/10.3390/land14081543>
- [17] Jongman, B., Kreibich, H., Apel, H., Barredo, J.I., Bates, P.D., Feyen, L., et al. (2012) Comparative Flood Damage Model Assessment: Towards a European Approach. *Natural Hazards and Earth System Sciences*, **12**, 3733-3752. <https://doi.org/10.5194/nhess-12-3733-2012>
- [18] Süzen, M.L. and Doyuran, V. (2004) A Comparison of the GIS Based Landslide Susceptibility Assessment Methods: Multivariate versus Bivariate. *Environmental Geology*, **45**, 665-679. <https://doi.org/10.1007/s00254-003-0917-8>
- [19] Valjarević, A., Popovici, C., Štilić, A. and Radojković, M. (2022) Cloudiness and Water from Cloud Seeding in Connection with Plants Distribution in the Republic of Moldova. *Applied Water Science*, **12**, Article No. 262.

<https://doi.org/10.1007/s13201-022-01784-3>

- [20] Waseem, M., Ahmad, S., Ahmad, I., Wahab, H. and Leta, M.K. (2023) Urban Flood Risk Assessment Using AHP and Geospatial Techniques in Swat Pakistan. *SN Applied Sciences*, **5**, Article No. 215. <https://doi.org/10.1007/s42452-023-05445-1>
- [21] Westra, S., Fowler, H.J., Evans, J.P., Alexander, L.V., Berg, P., Johnson, F., *et al.* (2014) Future Changes to the Intensity and Frequency of Short-Duration Extreme Rainfall. *Reviews of Geophysics*, **52**, 522-555. <https://doi.org/10.1002/2014rg000464>
- [22] Sendek, A., Kretz, L., van der Plas, F., Seele-Dilbat, C., Schulz-Zunkel, C., Vieweg, M., *et al.* (2021) Topographical Factors Related to Flooding Frequency Promote Ecosystem Multifunctionality of Riparian Floodplains. *Ecological Indicators*, **132**, Article ID: 108312. <https://doi.org/10.1016/j.ecolind.2021.108312>
- [23] Quagliolo, C., Comino, E. and Pezzoli, A. (2021) Experimental Flash Floods Assessment through Urban Flood Risk Mitigation (UFRM) Model: The Case Study of Ligurian Coastal Cities. *Frontiers in Water*, **3**, Article ID: 663378. <https://doi.org/10.3389/frwa.2021.663378>